

This work is licensed under a Creative Commons Attribution License (CC BY 4.0).

Research article

<urn:lsid:zoobank.org:pub:4C7F00E0-9567-4E1D-8CAB-AB3724537DC9>

Morphological and molecular analysis of *Willowsia nigromaculata* (Collembola, Entomobryidae, Entomobryinae) reveals a new cryptic species from the United States

Nikolas G. CIPOLA^{1,*} & Aron D. KATZ²

¹Laboratório de Sistemática e Ecologia de Invertebrados do Solo, Instituto Nacional de Pesquisas da Amazônia – INPA, CPEN. Av. André Araújo, 2936, Aleixo, CEP 69067–375, Manaus, AM, Brazil.

²Engineer Research and Development Center, 2902 Newmark Drive, Champaign, IL 61826, USA.

²Illinois Natural History Survey, Prairie Research Institute, University of Illinois at Urbana-Champaign, 1816 South Oak Street, Champaign, IL 61820, USA.

*Corresponding author: nikolasgc@gmail.com

²Email: aronkatz@illinois.edu

¹<urn:lsid:zoobank.org:author:70DD3D02-82A6-466D-B222-8A30DF9D933F>

²<urn:lsid:zoobank.org:author:72328BBA-0AF8-41D9-813C-A21EEC7C90C5>

Abstract. Commonly reported as a household pest throughout the northern hemisphere, *Willowsia nigromaculata* (Lubbock) is among the most abundant and widely distributed springtails. However, taxonomic uncertainty due to incomplete morphological descriptions based on specimens from different continents may lead to incorrect identifications and/or prevent the recognition of distinct lineages within this morphospecies. Here, we perform the first comprehensive morphological and genetic comparison between *W. nigromaculata* specimens collected from North America and Europe. Morphological and genetic evidence reveals that populations in the United States and France represent two distinct *nigromaculata*-like species, but a phylogenetic analysis indicates both species may also be present in Canada. Based on these results, we redescribe *W. nigromaculata* from France, provide a description for *Willowsia neonigromaculata* sp. nov. from the United States, and propose new diagnostic characters for their separation, including the number of inner appendages on the maxillary sublobal plate. We also highlight the need for morphological and molecular investigations of additional populations to better understand the diversity and distribution of *W. nigromaculata* and related species.

Keywords. Chaetotaxy, phylogeny, new species, Willowsiinae, *Willowsia neonigromaculata* sp. nov.

Cipola N.G. & Katz A.D. 2021. Morphological and molecular analysis of *Willowsia nigromaculata* (Collembola, Entomobryidae, Entomobryinae) reveals a new cryptic species from the United States. *European Journal of Taxonomy* 739: 92–116. <https://doi.org/10.5852/ejt.2021.739.1269>

Introduction

Originally described as *Seira nigromaculata* Lubbock, 1873, and later designated as the type species for the genus *Willowsia* Shoeborthan, 1917, *Willowsia nigromaculata* (Lubbock, 1873) is considered to be

among the most abundant and widely distributed species of Collembola, occurring in human structures such as homes, cellars, windowsills, greenhouses, and grain silos throughout the northern hemisphere (Guthrie 1903; Maynard 1951; Scott 1991; Christiansen & Bellinger 1998; Fjellberg 2007; Zhang *et al.* 2011; Bellinger *et al.* 2020). Despite being a common household and agricultural pest, the taxonomic status of this species remains uncertain.

Until recently, *W. nigromaculata* was identified primarily by color pattern (Gisin 1960; Stach 1967; Fjellberg 2007), especially in North America (Guthrie 1903; Maynard 1951; Christiansen & Bellinger 1998). Color pattern has been shown to be a useful species-level diagnostic character in certain cases (Soto-Adames 2002; Katz *et al.* 2015a; Ding *et al.* 2018), but other studies also highlight the importance of including chaetotaxy and other morphological characters, in addition to color pattern, for Entomobryinae species diagnosis (Jordana 2012; Katz *et al.* 2015b). Szeptycki (1979), Christiansen & Bellinger (1980), and Zhang *et al.* (2011) provided modern descriptions of dorsal chaetotaxy for populations of *W. nigromaculata* in Poland, United States of America (USA), and France, respectively, but many important characters were not revealed, including head chaetotaxy, mouthparts, collophore and manubrium. Katz (2017) later provided descriptions of some of these missing characters based on specimens collected in the USA but did not examine European material for comparison.

Incomplete species descriptions of *W. nigromaculata* based on specimens collected from different continents may prevent the recognition of distinct species, and consequently, species identifications could be misleading and/or populations may be incorrectly assumed to be introduced on other continents. In response to this concern, we conduct the first comprehensive morphological and genetic comparisons of *W. nigromaculata* with specimens collected from both North America and Europe to (1) determine whether morphologically and/or genetically distinct lineages are present within *W. nigromaculata*, (2) determine if morphological and/or genetic differences correspond to collection locality, (3) provide taxonomic redescriptions of *W. nigromaculata* and any potential new species and (4) reveal new diagnostic characters for the identification of any distinct lineages uncovered within *W. nigromaculata*.

Material and methods

Morphological analysis

Specimens preserved in 92–95% ethanol and identified as *Willowsia nigromaculata* from Paris, France and Illinois, USA, were cleared with Nesbitt's solution and then mounted on glass slides in Hoyer's medium following the procedures described by Jordana *et al.* (1997) in preparation for light microscopy. Specimens in ethanol gel were photographed using a stereo microscope M165C attached to a DFC420 digital camera with a dome as presented in Kawada & Buffington (2016). Photographs were digitized using Application Suite ver. 3.4.1. For scanning electron microscopy (SEM), specimens were transferred to absolute ethanol and critical point dried after sputter-coating with gold using the equipment BAL-TEC CPD 030 and BAL-TEC SPD 050, respectively. The images were made using a LEO VP 435 scanning electron microscope. The material is deposited in the Invertebrate Collection of the National Institute of Amazonian Research (INPA), Brazil, and the Illinois Natural History Survey (INHS) in Champaign, IL, United States.

The terminology used in descriptions mainly follows: clypeal chaetotaxy after Yoshii & Suhardjono (1992); labral chaetotaxy after Cipola *et al.* (2014); labial papillae, maxillary palp and basolateral and basomedian labial fields after Fjellberg (1999), using Gisin's system (1967) to a 1–5 chaetae labels; postlabial chaetotaxy after Chen & Christiansen (1993); subcoxae outer chaetotaxy after Yosii (1959); and unguiculus lamellae after Hüther (1986). The head dorsal chaetotaxy follows Mari-Mutt (1979) and

body after Szeptycki (1979), both adapted from Soto-Adames (2008) and Katz (2017); and specialized chaetae (S-chaetae) after Zhang & Deharveng (2015). Macrochaetotaxy simplified formula follows Gisin (1967) and Cipolla *et al.* (2020) with modifications. Symbols used to depict the chaetotaxy are presented in Figure 1. Chaetae of uncertain homology are followed by a question mark (?). Chaetotaxy all given left side of body only.

Abbreviations

Abd I–VI	=	abdominal segments
ae	=	antero-external lamella
ai	=	antero-internal lamella
Ant I–IV	=	antennal segments
a.t.	=	apical tooth of unguis
b.c.	=	basal chaeta
b.t.	=	basal tooth of unguis
l.p.	=	lateral process of labial papilla E
mac	=	macrochaeta, -ae
mes	=	mesochaeta, -ae
m.t.	=	apical tooth of unguis
pe	=	postero-external lamella
pi	=	postero-internal lamella
psp	=	pseudopore, -es
ms	=	specialized microchaeta
sb.	=	sublobal chaetae
sens	=	specialised ordinary chaetae, -ae
Th II–III	=	thoracic segments
t.a.	=	terminal appendage

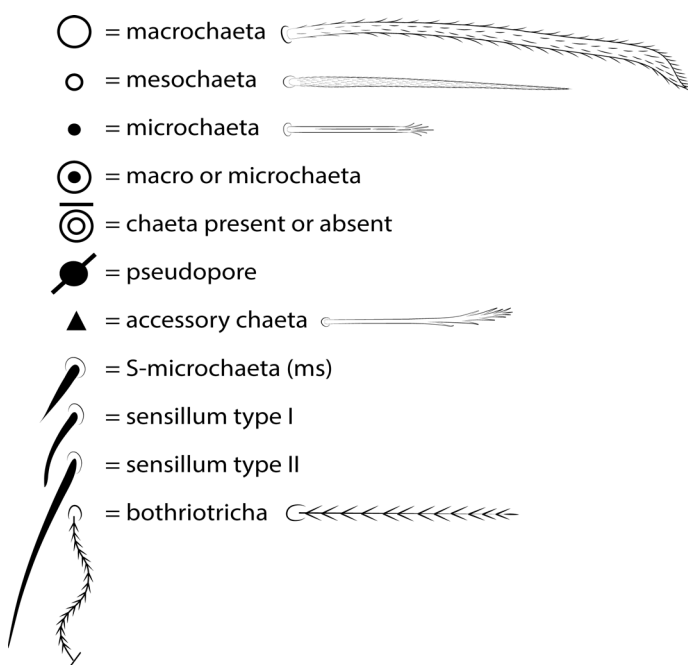


Fig. 1. Symbols used in dorsal chaetotaxy description of species of *Willowsia* Shoebghan, 1917.

Genetic analysis

Forty mitochondrial cytochrome oxidase subunit 1 (COI) gene sequences, representing ten Entomobryinae genera, were downloaded from NCBI GenBank and used for genetic analysis (Table 1). Genetic variation within *W. nigromaculata* was evaluated using sequences of six specimens identified as *W. nigromaculata*: one from Dixon Springs Agricultural Center, Pope County, Illinois, USA (Katz *et al.* 2015a, 2015b); one from Teillet, France (Ding *et al.* 2018); one from Brockville, Canada (deWaard *et al.* 2019); and three from Toronto, Canada (deWaard *et al.* 2019). To provide a more comprehensive approach for assessing genetic variation within Entomobryinae, a subfamily rife with para- and polyphyletic genera (Zhang *et al.* 2014a, 2014b, 2015, 2016, 2017; Katz *et al.* 2015b, 2017; Zhang & Deharveng 2015; Ding *et al.* 2018), we augmented our dataset with species from the Entomobryinae genera *Coecobyra* (1), *Drepanura* (1), *Entomobrya* (16), *Entomobryoides* (1), *Homidia* (2), *Lepidodens* (1), and *Sinhomidia* (1), in addition to other *Willowsia* species (8). Lastly, we included three species in the genera *Lepidocyrtoides* (2) and *Lepidosira* (1) to serve as phylogenetic outgroups as they have been shown to comprise the sister lineage to all other Entomobryinae (Nunes *et al.* 2019; Godeiro *et al.* 2020). Sequences were aligned using the G-INSI-i alignment method implemented in MAFFT ver. 7.273 (Katoh & Standley 2013).

Uncorrected pairwise COI distances were calculated in Geneious Prime ver. 2020.0.4 (<https://www.geneious.com>) and plotted in R ver. 3.6.3 (R Core Team 2020) to (1) characterize genetic variation within *W. nigromaculata*, (2) compare the genetic variation within *W. nigromaculata* with variation observed between other species of Entomobryinae, and (3) identify potential gaps in the distribution of genetic variation which may indicate the presence of both inter- and intra-specific variation within *W. nigromaculata*.

Bayesian and maximum likelihood approaches were employed to estimate phylogenetic relationships among Entomobryinae species to determine if distinct and divergent lineages are present within *W. nigromaculata* and if they correspond with differences in collection locality and/or morphology. PartitionFinder2 ver. 2.2.1 (Lanfear *et al.* 2017) was used to determine the appropriate models of sequence evolution and partitioning scheme. Bayesian analysis was performed using MrBayes ver. 3.2.7 (Ronquist *et al.* 2012) with the following parameters: codon positons 1–3 were partitioned separately with GTR+I+G, GTR+I+G, and GTR+G site models, respectively; ingroup taxa were constrained to be monophyletic; Markov chain Monte Carlo (MCMC) for 200 million generations; samplefreq = 1,000; and nrungs = 2. Convergence was assessed by observation of average split frequencies values below $p < 0.004$. A 50% Bayesian consensus tree was generated combining both runs using the sumt command with a 25% burn-in. We also performed an additional Bayesian analysis using BEAST2 ver. 2.6.2 (Bouckaert *et al.* 2019) with the following parameters: codon positions 1–3 were partitioned separately for site model averaging with the bModelTest package (Bouckaert & Drummond 2017); a strict clock rate set to 1 for relative branch length estimation; Yule tree model; monophyletic constraint prior on ingroup taxa; MCMC for 200 million generations; and sampling trees and statistics every 1000 generations. After a 10% burn-in, effective sample size (ESS) for all parameters was determined to be greater than 200 with Tracer ver. 1.7.1 (Rambaut *et al.* 2018). A maximum clade credibility tree was estimated using TreeAnnotator ver. 2.6.0 (Bouckaert *et al.* 2019) with median node heights and a 10% burn-in. Maximum likelihood analysis was performed with RAxML-NG ver. 9.0 (Kozlov *et al.* 2019) using the all-in-one ML search and bootstrapping command (all), a partition file treating codon positions 1–3 as separate partitions with the same site models used for the MrBayes analysis, a constraint tree forcing monophly for ingroup taxa, scaled branch lengths, and MRE-based bootstrapping (converged after 400 replicates).

Table 1 (continued on next page). List of Entomobryinae species used for phylogenetic analysis, including locality and COI sequence information, i.e., GenBank accession number and sequence length (bp = base pairs). Abbreviations: AH = Anhui; AL = Alabama; AM = Amazonas; AZ = Azores; BA = Bahia; BR = Brazil; CA = Canada; CH = China; FL = Florida; FR = France; GD = Guangdong; HB = Hubei; HN = Hunan; IDF = Île-de-France; IL = Illinois; JL = Jilin; NC = North Carolina; OOC = Occitanie; ON = Ontario; PA = Pennsylvania; PI = Piauí; PT = Portugal; TB = Tibet; TN = Tennessee; USA = United States of America; VT = Vermont; WI = Wisconsin; ZJ = Zhejiang.

	Species name	Locality	GenBank #	bp	Reference
1	<i>Coecobrya tenebricosa</i>	Antony, IDF, FR	KM978347	658	Ding <i>et al.</i> 2018
2	<i>Drepanura mogolica</i>	Changling, JL, CH	KY468329	658	Ding <i>et al.</i> 2018
3	<i>Entomobrya assuta</i>	Mason Co., IL, USA	KM610057	1534	Katz <i>et al.</i> 2015a
4	<i>Entomobrya atrocincta</i>	Champaign Co., IL, USA	KM610115	1534	Katz <i>et al.</i> 2015a
5	<i>Entomobrya bicolor</i>	Henderson Co., IL, USA	KM610117	1534	Katz <i>et al.</i> 2015a
6	<i>Entomobrya citrensis</i>	Citrus Co., FL, USA	KM610064	1534	Katz <i>et al.</i> 2015a
7	<i>Entomobrya clitellaria</i>	Coles Co., IL, USA	KM610076	1534	Katz <i>et al.</i> 2015a
8	<i>Entomobrya decemfasciata</i>	Stewart Co., TN, USA	KM610101	1534	Katz <i>et al.</i> 2015a
9	<i>Entomobrya huangi</i>	Nyingchi, TB, CH	KY468314	658	Ding <i>et al.</i> 2018
10	<i>Entomobrya intermedia</i>	Chester Co., PA, USA	KM610121	1534	Katz <i>et al.</i> 2015a
11	<i>Entomobrya jubata</i>	Covington Co., AL, USA	KM610110	1534	Katz <i>et al.</i> 2015a
12	<i>Entomobrya ligata</i>	Swain Co., NC, USA	KM610079	1534	Katz <i>et al.</i> 2015a
13	<i>Entomobrya multifasciata</i>	São Miguel Island, AZ, PT	KM610123	1534	Katz <i>et al.</i> 2015a
14	<i>Entomobrya neotenica</i>	Clay Co., AL, USA	KM610104	1534	Katz <i>et al.</i> 2015a
15	<i>Entomobrya nivalis</i>	Lamoille Co., VT, USA	KM610125	1534	Katz <i>et al.</i> 2015a
16	<i>Entomobrya quadrilineata</i>	Vermilion Co., IL, USA	KM610092	1534	Katz <i>et al.</i> 2015a
17	<i>Entomobrya unifasciata</i>	Chester Co., PA, USA	KM610087	1534	Katz <i>et al.</i> 2015a
18	<i>Entomobrya unostrigata</i>	Champaign Co., IL, USA	MT454111	1530	Katz <i>et al.</i> 2015b
19	<i>Entomobryoides dissimilis</i>	Champaign Co., IL, USA	KM610126	1534	Katz <i>et al.</i> 2015a
20	<i>Homidia sauteri</i>	Butler Co., AL, USA	KM610127	1501	Katz <i>et al.</i> 2015a
21	<i>Homidia socia</i>	Jo Davies Co., IL, USA	KM610128	1534	Katz <i>et al.</i> 2015a
22	<i>Lepidocyrtoides caeruleomaculatus</i>	Rio Preto da Eva, AM, BR	MF716618	1534	Godeiro <i>et al.</i> 2020
23	<i>Lepidocyrtoides</i> sp.	Abaíra, BA, BR	MF716598	1534	Godeiro <i>et al.</i> 2020
24	<i>Lepidodens similis</i>	Shaoguan, GD, CH	KM978396	658	Ding <i>et al.</i> 2018
25	<i>Lepidosira neotropicalis</i>	Piracuruca, PI, BR	MF716603	1534	Nunes <i>et al.</i> 2019
26	<i>Sinhomidia bicolor</i>	Huangshan, AH, CH	KM978375	658	Ding <i>et al.</i> 2018
27	<i>Willowsia buski</i>	Sauk Co., WI, USA	KM610129	1534	Katz <i>et al.</i> 2015a
28	<i>Willowsia fascia</i>	Huanggang, HB, CH	KU833222	658	Ding <i>et al.</i> 2018
29	<i>Willowsia guangdongensis</i>	Guangzhou, GD, CH	KM978377	658	Ding <i>et al.</i> 2018
30	<i>Willowsia japonica</i>	Linhai, ZJ, CH	KM978378	658	Ding <i>et al.</i> 2018
35	<i>Willowsia neonigromaculata</i> sp. nov.	Pope Co., IL, USA	KM610130	1534	Katz <i>et al.</i> 2015a
36	<i>Willowsia neonigromaculata</i> sp. nov.	Brockville, ON, CA	MG034057	542	deWaard <i>et al.</i> 2019
31	<i>Willowsia nigromaculata</i>	Teillet, OCC, FR	KY468311	658	Ding <i>et al.</i> 2018
32	<i>Willowsia nigromaculata</i>	Toronto, ON, CA	MG032239	474	deWaard <i>et al.</i> 2019
33	<i>Willowsia nigromaculata</i>	Toronto, ON, CA	MG036766	594	deWaard <i>et al.</i> 2019
34	<i>Willowsia nigromaculata</i>	Toronto, ON, CA	MG039377	543	deWaard <i>et al.</i> 2019
37	<i>Willowsia pseudobuski</i>	Lu'an, AH, CH	KU833223	658	Ding <i>et al.</i> 2018

Table 1 (continued).

Species name	Locality	GenBank #	bp	Reference
38 <i>Willowsia pyrrhopygia</i>	Citrus Co., FL, USA	KM610131	1534	Katz <i>et al.</i> 2015a
39 <i>Willowsia qui</i>	Huangshan, AH, CH	KU833221	658	Ding <i>et al.</i> 2018
40 <i>Willowsia similis</i>	Changsha, HN, CH	KU833225	658	Ding <i>et al.</i> 2018

Results

Taxonomic descriptions

The following characters are shared by both *Willowsia* species (described below) and are not repeated in the descriptions: scales apically pointed with long basal ribs covering $\frac{2}{3}$ of scale and present dorsally on head, thorax and abdomen (Figs 2–3A, 8); antenna, ventral head, legs, collophore and furcula unscaled (Figs 3D, 4, 7); mac heavily ciliate, apically truncate or acuminate (Fig. 1); mic basally smooth with longer ramificate ribs from distal half (Figs 1, 3B); bothriotricha accessory chaeta with short ramificate ribs distally (Figs 1, 3C, 6D–F); antenna less than the trunk length (Figs 2, 8); Ant III distally with 2 apical organ somewhat elongated, 3 spiny guard sensilla, s-blunt sens of different sizes and ciliate chaetae (Fig. 5A); eyes 8+8, A and B larger, G and H smaller (Figs 5B, 9A); clypeal formula with 4 (11–2), 7 (f), 3 (pf0–1) ciliate chaetae, 11–2 and pf1 larger, 4 frontal chaetae smaller, others subequal; four prelabral chaetae ciliate; labral formula with 4 (a1–2), 5 (m0–2), 5 (p0–2) smooth chaetae, p0–1 larger, others subequal (Fig. 5C); four labral papillae apically pointed and subequal (Fig. 5D); labial palp with 5 main (A–E) and 1 hypostomal papilla (H), with 0, 5, 0, 4, 4, 2 guard appendages, respectively, l.p. of papilla E gently pointed and exceeds base of apical appendage (Fig. 5F); labium with 5 smooth proximal chaetae; basomedian and basolateral labial fields with a1–5 smooth, M, R (smaller), E, L1–2 ciliate (Fig. 5G); Th II–Abd V with ms and sens formula 1,0|1,0,1,0,0 and 2,2|1,2,2,+3, respectively; Abd II–IV bothriotricha formula 2 (a5 and m2), 3 (a5, m2, and m5), and 2 (T2 and T4), respectively (Fig. 6); Tibiotarsus I–III sometimes subdivided on distal two thirds; tibiotarsus III distally with 1 inner smooth chaeta and 1 outer tenent hairs capitate and heavily ciliate (Figs 3D–E, 7E); pretarsus with 1 minute smooth chaeta on anterior and posterior sides (Figs 3D, 7E); unguis inner side with 4 inner teeth, b.t. paired and of same length than m.t., a.t. smaller; outer side with 2 paired basolateral teeth and 1 unpaired basomedian tooth, all with one lamella which extends to the base; unguiculus with four lamellae, ae, ai and pi acuminate and smooth, and pe serrated (Figs 3D–E, 7E); Mucro bidentate, proximal tooth gently smaller than distal, basal spine reaches apex of proximal tooth (Figs 3F, 7J).

Family Entomobryidae Schäffer, 1896

Subfamily Entomobryinae Schäffer, 1896 *sensu* Zhang & Deharveng 2015

Genus *Willowsia* Shoebottom, 1917

Willowsia nigromaculata (Lubbock, 1873)

Figs 2–7, 10–11; Tables 2–3

Seira nigromaculata Lubbock 1873: 146, Great Britain (orig. descr.).

Willowsia nigromaculata – Shoebottom 1917: 432 (comb.). — Zhang *et al.* 2011 (descr.).

Type species

Seira nigromaculata Lubbock, 1873.

Diagnosis

Body with pigments laterally on head to Abd III, and spots on Abd IV, femur and tibiotarsus (Fig. 2); head mac S0 absent, Ps3 mes and Ps5 mac present; sublobal plate with 2 inner appendages (Fig. 5E); Th II–Abd IV formula with $9,8|3,3,3+7,7+14$ mac, p2a rarely present on Th III (Fig. 6A–C); manubrium dorsally with 7 lateral chaetae abruptly acuminate at the tip, manubrial plate with 3–4 chaetae, 1 mac (Fig. 7G–H).

Material examined

FRANCE • 2 ♂♂, 5 ♀♀, 1 juvenile on slides, 7 specimens in alcohol; Paris, National Museum of Natural History, Department de Systematique et Évolution; $48^{\circ}50'30.0''$ N, $02^{\circ}21'33.1''$ E; in laboratory benchtop; 1 Jun. 2016; VD Tarli leg.; INPA.

Description

LENGTH. Total length (head + trunk) of specimens 1.51–1.85 mm ($n = 3$). Specimens pale yellowish white with violet pigments on Ant II to Ant IV, head laterally, margins of Th II–Abd II, Abd III with one transverse band that expands laterally, Abd IV dorsally with one irregular lateral spot, irregular spots on



Fig. 2. *Willowsia nigromaculata* (Lubbock, 1873), habitus. **A.** Lateral view. **B.** Dorsal view. Scale bars: 0.5 mm.

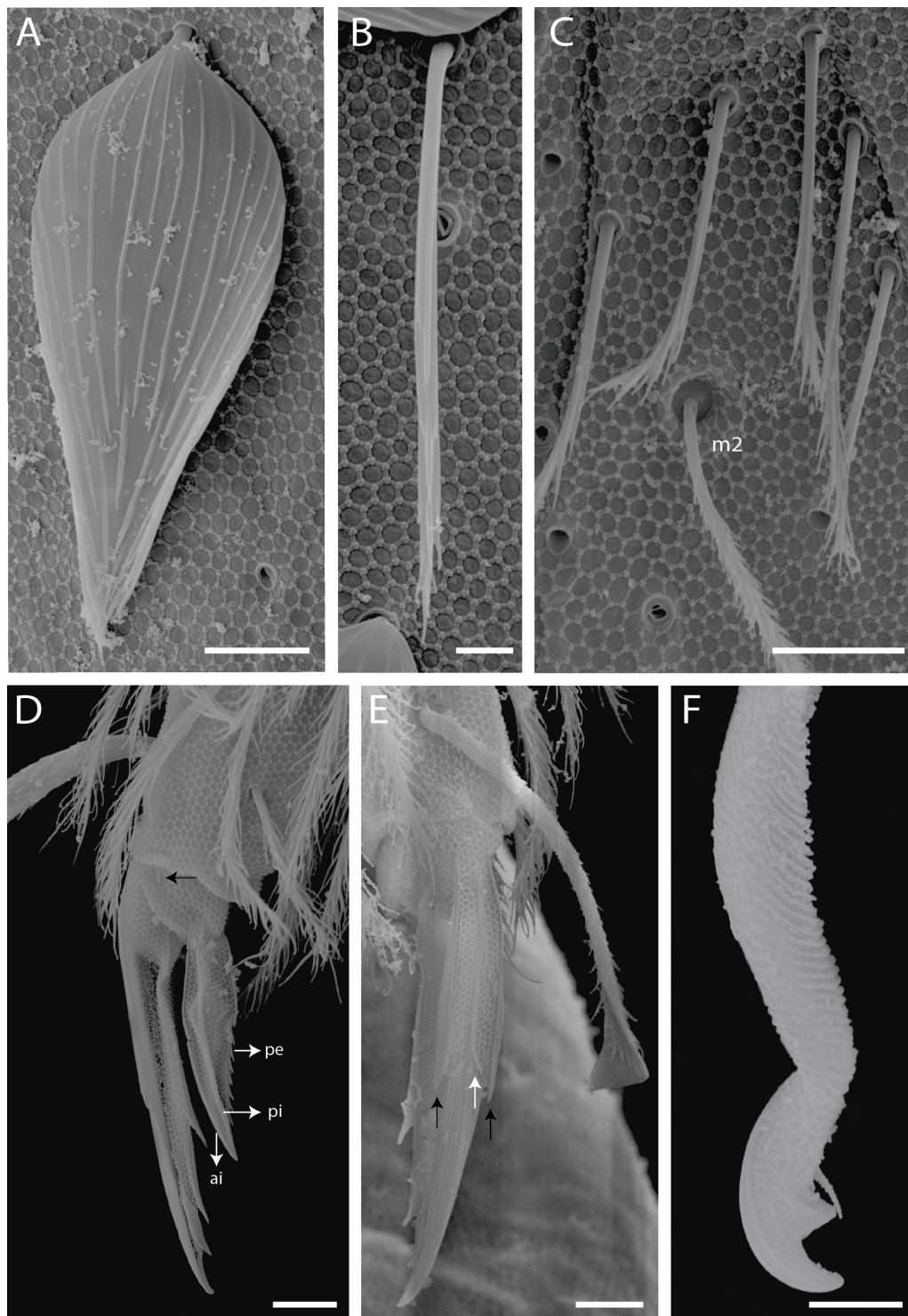


Fig. 3. Scanning electron microscopy of *Willowsia nigromaculata* (Lubbock, 1873). **A.** Scale apically pointed of Abd IV. **B.** Tergal microchaeta basally smooth and with ramification on distal half. **C.** Bothriotrichal complex of Abd II, m2 is bothriotrichum. **D.** Distal tibiotarsus and empodial complex I (posterior side), black arrow indicates pretarsal chaeta and white arrows indicates unguiculus lamellae. **E.** Distal tibiotarsus and empodial complex II (outer side), white arrow indicates unpaired basomedian tooth and black arrows indicates paired basolateral teeth of the unguis. **F.** Distal dens and mucro (lateral side). Abbreviations: see Material and methods. Scale bars: A, C–F = 5 µm; B = 2 µm.

dorsoventral plate and posterior border; distal half of Abd V to VI, distal femur and tibiotarsus medially; eyepatches black (Fig. 2).

HEAD. Antennal ratio as I: II: III: IV = 1: 1.83–2.00 1.68–2.12: 1.81–2.36 (n = 3). Ant IV not annulated, with apical bulb bilobed and sometimes retractile. Five interocular chaetae (q, v, p, r, t); head dorsal macrochaetotaxy (Fig. 5B) with 5 ‘An’ (An1a–3), 4 ‘A’ (A0, A2–3, A5), 3 ‘M’ (M1–2, M4), 6 ‘S’ (S2–6), 1 ‘Ps’ (Ps5), 5 ‘Pa’ (Pa1–5), 2 ‘Pm’ (Pm1, Pm3), 5 ‘Pp’ (Pp1–5), and 2 ‘Pe’ (Pe2–3) mac; An2a?, A1, A4? mic present. Maxillary palp with t.a. smooth and b.c. weakly striated, thicker and 1.12 longer than t.a.; sublobal plate with 2 inner (sb.2–3) and 1 outer (sb.4) smooth appendages, sb.2 smaller and sb.4 minute (Fig. 5E). Ventral chaetotaxy with about 68 ciliate chaetae, 36 thin of different sizes, 31 normal and subequal in length and 1 b.c., cephalic groove with 6 chaetae; postlabial formula with 4 (G1–4), 4 (X, X2–4), 4 (H2–4), 4 (J1–4), 2 (X’, X4’) chaetae (Fig. 5G).

THORAX CHAETOTAXY (Fig. 6A). Th II, anterior collar with numerous chaetae; a, m and p series with 1 (a5), 1 (m4) and 7 (p1–5) mac, respectively. Th III, a, m and p series with 2 (a4, a6), 4 (m5–7) and 5–6 (p1–3, p5–6) mac, respectively, p2a mac rarely present; laterally numerous mes. Ratio Th II: III = 1.48–1.30: 1 (n=3).

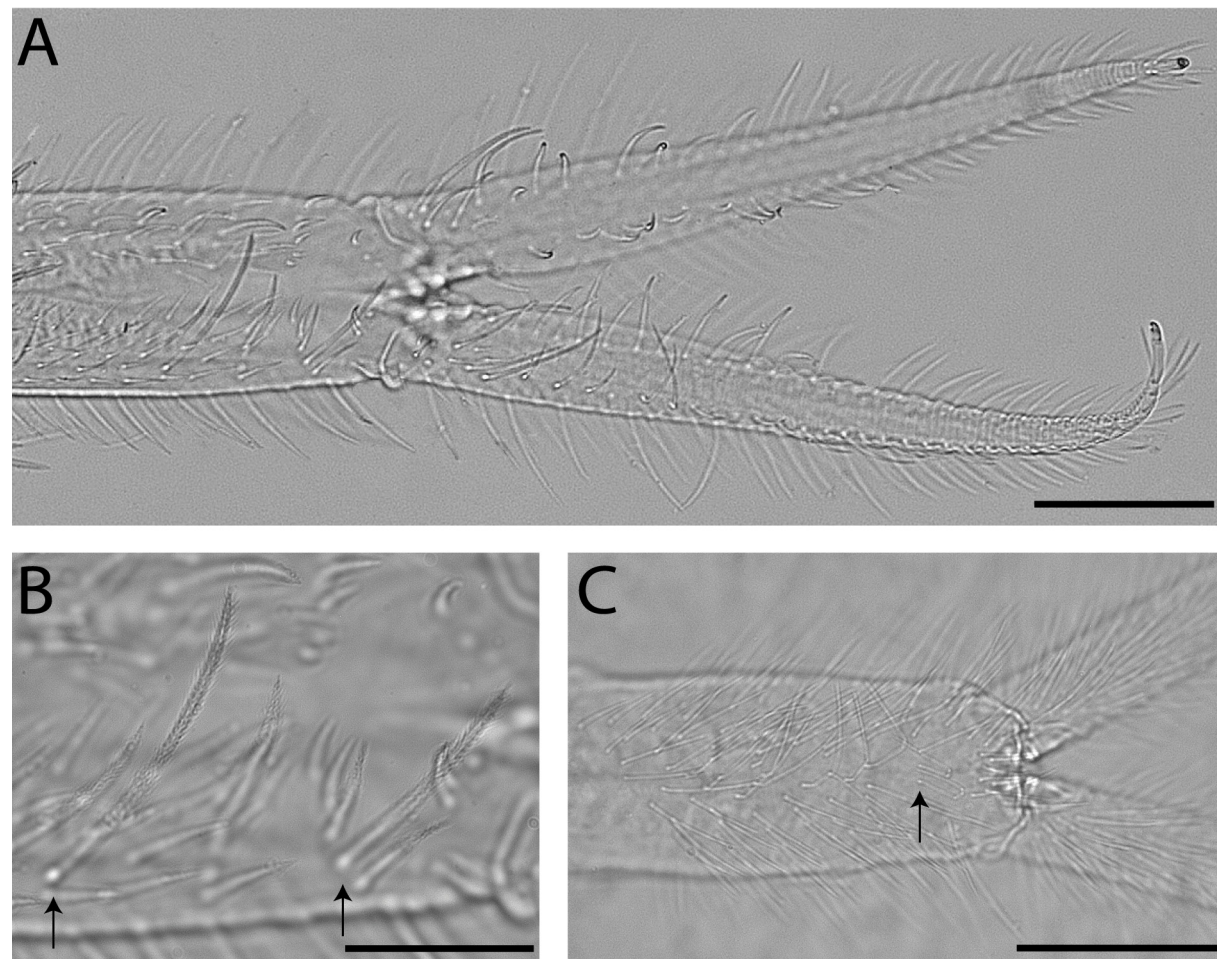


Fig. 4. Optical microscope photography of *Willowsia nigromaculata* (Lubbock, 1873). **A.** Furcula (dorsal view). **B.** Manubrium (dorsal view), arrows indicate mac and mes suddenly acuminate, respectively. **C.** Manubrium and proximal dentes (ventral view), arrow indicate subapical chaetae. Scale bars: A, C =100 µm; B = 50 µm.

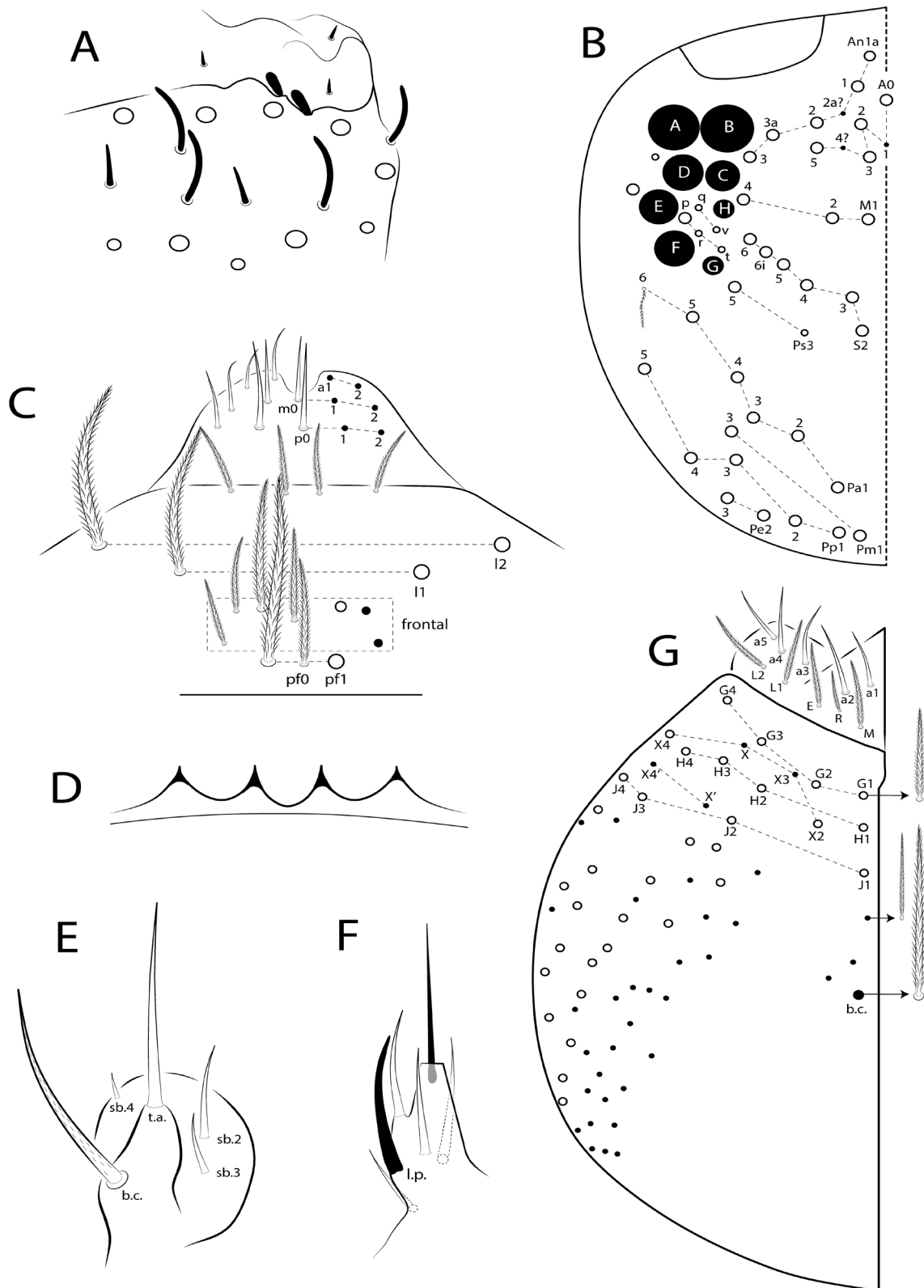


Fig. 5. *Willowsia nigromaculata* (Lubbock, 1873), head (left side). **A.** Ant III apical organ. **B.** Cephalic dorsal chaetotaxy. **C.** Chaetotaxy of clypeus, prelabrum and labrum. **D.** Labral papillae. **E.** Maxillary outer lobe. **F.** Papilla E of labial palp (ventral view). **G.** Basomedian and basolateral labial fields and complete postlabial chaetotaxy. Abbreviations: see Material and methods.

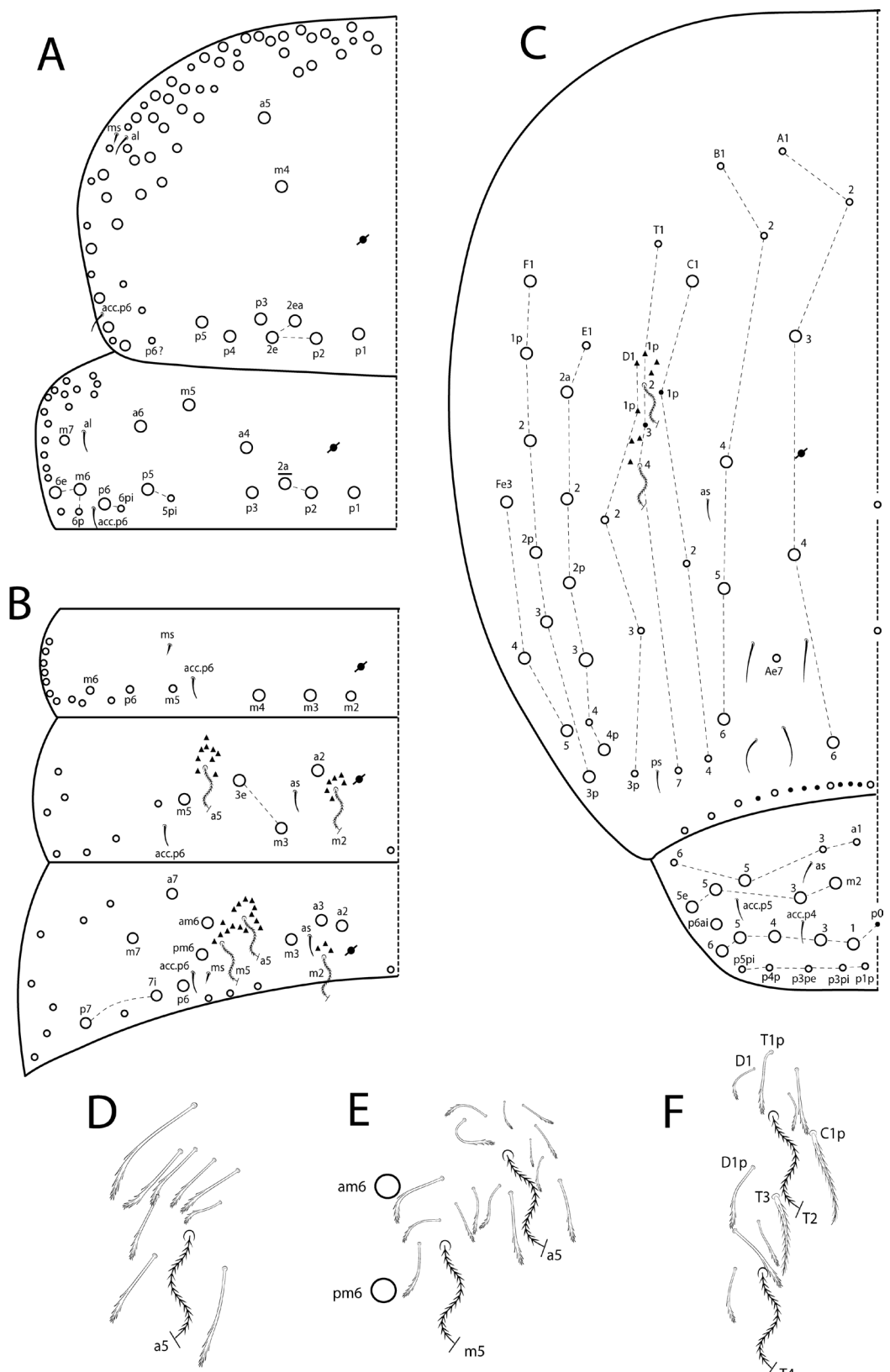


Fig. 6. *Willowsia nigromaculata* (Lubbock, 1873), dorsal chaetotaxy (left side). **A.** Th II–III. **B.** Abd I–III. **C.** Abd IV–V. **D–F.** Bothriotrichal complex. **D.** Abd II. **E.** Abd III. **F.** Abd IV. Abbreviations: see Material and methods.

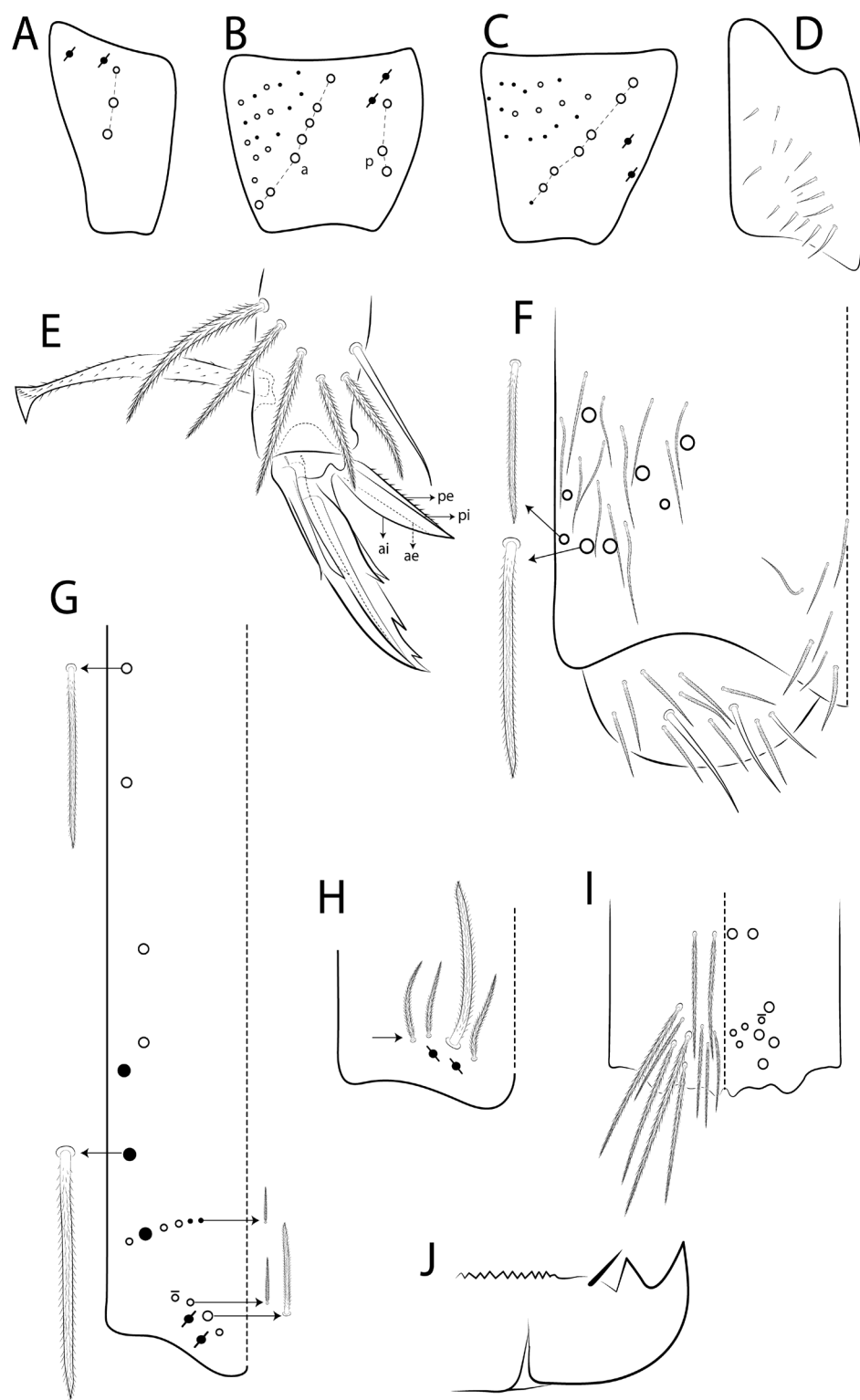


Fig. 7. *Willowsia nigromaculata* (Lubbock, 1873). **A.** Subcoxa I. **B.** Subcoxa II. **C.** Subcoxa III (lateral view). **D.** Trochanteral organ. **E.** Distal tibiotarsus and empodial complex III (posterior view). **F.** Collophore chaetotaxy (lateral view). **G.** Manubrium dorsal chaetotaxy. **H.** Manubrial plate. **I.** Subapical and apical chaetotaxy of ventral manubrium. **J.** Mucro (lateral view). Abbreviations: see Material and methods.

ABDOMEN CHAETOTAXY (Fig. 6B–F). Abd I, m series with 3 mac (m2–4) subequal in length. Abd II, a and m series with 1 (a2) and 3 (m3–3e, m5) mac, respectively; a5 and m2 bothriotricha with 9 and 6 accessory chaetae, respectively (Figs 3C, 6D). Abd III, a, m and p series with 3 (a2–3, a7), 4 (m3, am6, pm6, m7) and 3 (p6, p7–7i) mac, respectively; m2 bothriotrichum with 3 accessory chaetae and a5 and m5 bothriotricha with 15 accessory chaetae between them (Fig. 6E). Abd IV, A to T series with 7 mac (A3–4, A6, B4–6, C1) and E to Fe series with 14 mac (E2a–3, E4p, F1–3p, Fe3–5); T2 and T4 bothriotricha with 2 mic and 8 accessory chaetae between them (Fig. 6F); 2 sens type I (as, ps), 4 sens type II, and 13 posterior chaetae of different sizes. Abd V a, m, pa and p series with 1 (a5), 4 (m2–3, m5–5e), 1 (p6ai) and 5 (p1, p3–6) mac, respectively. Ratio Abd III: IV = 1: 3.61–4.14 (n= 3).

LEGS. Subcoxa I with 3 chaetae and 2 psp; subcoxa II with an anterior row of 7 chaetae and about 16 anterior chaetae, posterior row of 3 chaetae and 2 psp; subcoxa III with one row of 7 chaetae, about 16 anterior chaetae and 2 posterior psp (Fig. 7A–C). Trochanteral organ with 12–16 spine-like chaetae (Fig. 7D). Ratio unguis: unguiculus = 1: 0.52. Tibiotarsal smooth chaeta 1.09 the length of unguiculus; tenent hairs 0.97 the length of unguis.

COLLOPHORE. Anterior side with about 20 chaetae, 5 mac and 3 mes ciliate and abruptly acuminate at the tip, and 13 thin chaetae weakly ciliate; posterior side with 8 chaetae (1 unpaired) weakly ciliate and 2 distally thicker; lateral flap with 3 smooth chaetae and 9 chaetae weakly ciliate (Fig. 7F).

FURCULA. Manubrium ventrally with 4 subapical chaetae of the same length and 14–16 apical chaetae, 6 inner chaetae smaller, others subequal (Figs 4C, 7I); dorsally with one lateral row of 7 ciliate chaetae abruptly acuminate at the tip, 3 mac and 4 mes (1 basal and 1 antero-subapical); manubrial plate with 3–4 ciliate chaetae of different sizes (1 mac abruptly acuminate at the tip) and 2 psp (Figs 4A–B, 7G–H).

DNA Barcodes

GenBank KY468311; Teillet, France (Ding *et al.* 2018). GenBank MG032239, MG036766, MG039377; Toronto, Canada (deWaard *et al.* 2019).

Willowsia neonigromaculata sp. nov. Katz & Cipolla
[urn:lsid:zoobank.org:act:195E3CC7-B9AB-4CE9-93DE-BBA8ABA443C9](https://doi.org/10.1545/zobt.195E3CC7-B9AB-4CE9-93DE-BBA8ABA443C9)
Figs 8–11; Tables 2–3

Willowsia nigromaculata – Katz 2015a: 829, Illinois, USA (phylogeny). — Katz 2015b: 64, Illinois, USA (phylogeny). — Katz 2017: 553, Illinois, USA (descr.). — deWaard *et al.* 2019: suppl. data, Brockville, Canada (DNA barcode, GenBank MG034057).

Diagnosis

Body with pigments laterally on head to Abd III, and spots on Abd IV, femur and tibiotarsus (Fig. 8), sometimes with piment covering nearly all Abd II–III medially and posterior half of Abd IV; head mac S0 present or absent, Ps3 mes and Ps5 mac absent (Fig. 9A); sublobal plate with 3 inner appendages (Fig. 9B); Th II–Abd IV formula with 9,8|3,3,3+7,7+14 mac, p2a present on Th III; manubrium dorsally with 9 lateral chaetae abruptly acuminate at the tip, manubrial plate with 4 chaetae, 2 mac (Fig. 9E).

Etymology

The specific epithet is derived from the Greek adjective ‘νέος, -α, -ον’, Latinized ‘neos, -a, -um’ (combining form *neo-*), ‘new, recent, young’ + the epithet of the species *Willowsia nigromaculata*

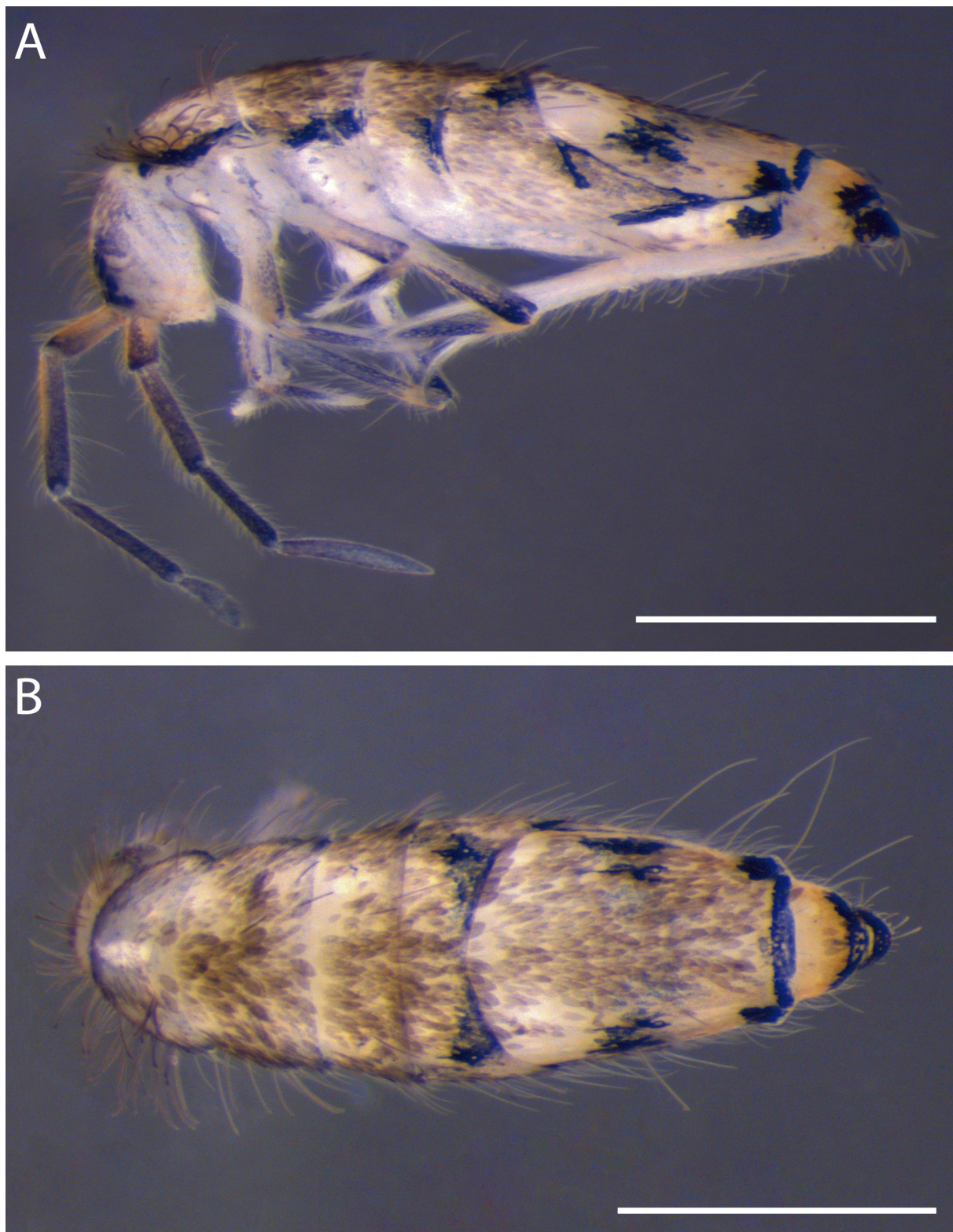


Fig. 8. *Willowsia neonigromaculata* sp. nov., paratype, ♀ (INHS 810158), habitus. A. Lateral view. B. Dorsal view. Scale bars: 0.5 mm.

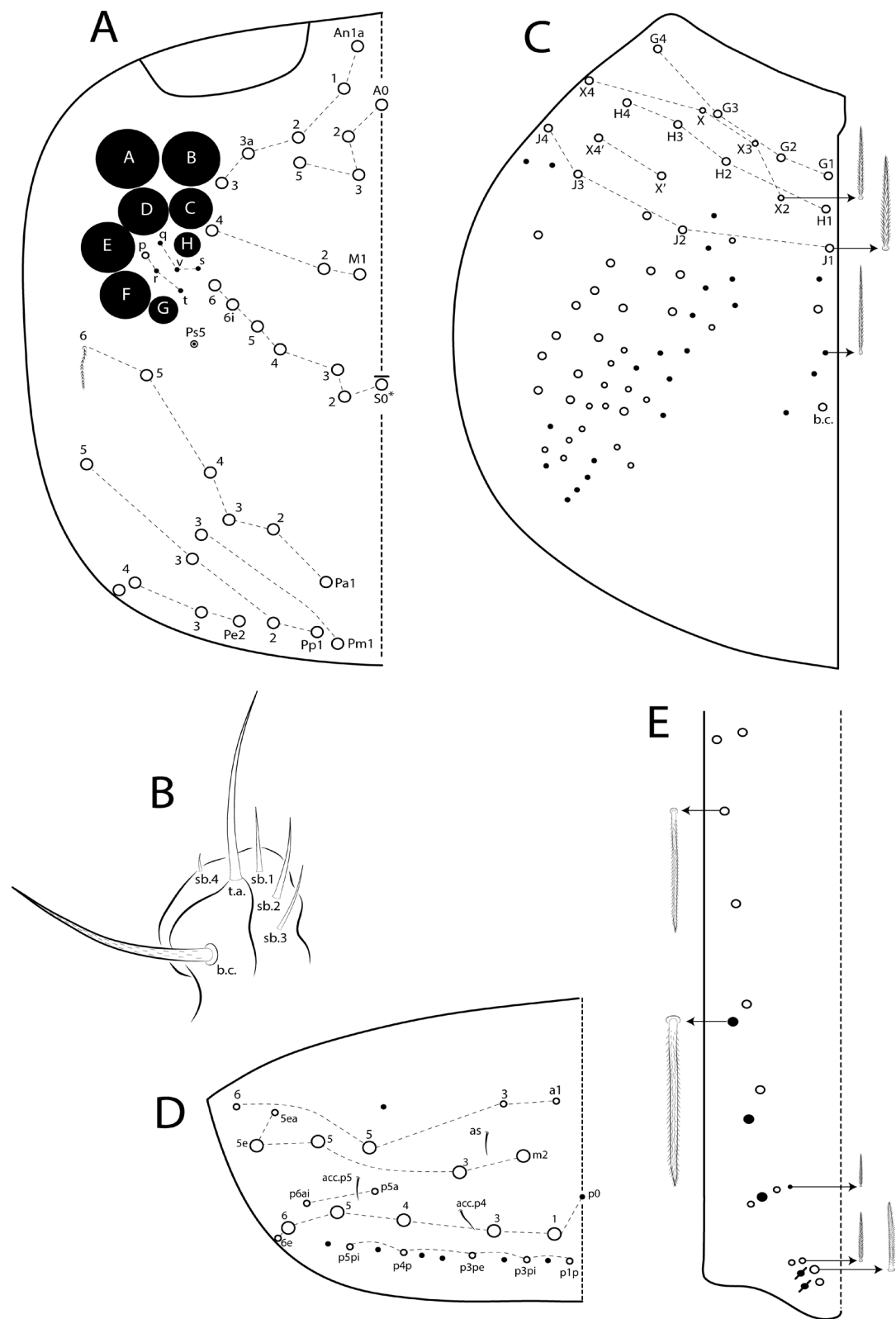


Fig. 9. *Willowsia neonigromaculata* sp. nov., body parts (left side). **A.** Cephalic dorsal chaetotaxy. **B.** Maxillary outer lobe. **C.** Complete postlabial chaetotaxy. **D.** Abd V dorsal chaetotaxy. **E.** Manubrium dorsal chaetotaxy. Abbreviations: see Material and methods.

(Lubbock, 1873). The name references the new species' morphological affinity with *W. nigromaculata* and its presence in the New World.

Material examined

Holotype

USA • 1 ♀ on slide; Illinois, Pope Co., Dixon Springs Agricultural Center; 37°26'03.65" N, 88°40'01.84" W; altitude 524 m, hand collected on pavement on dying *Arilus cristatus*; 23 Sep. 2011; A. Katz leg.; adk11-159; INHS 810161.

Paratypes

USA • 1 ♂, 2 ♀, 2 undetermined sex on slides and 30 specimens in alcohol; same data as for holotype; INHS 810157–810160, INHS 810162, INHS 810163.

Other material

USA • 1 undetermined sex on slide; Illinois, Urbana, 19 Montclair Rd; 40°05'41.5" N, 88°12'24.7" W; 6 Jul. 2008; by kitchen sink; F Soto-Adames leg.; INHS 810,164 • 2 ♀♀ on slide; same collection data as for preceding, except 2012 (no specific date); INHS 810165.

Description

LENGTH. Total length (head + trunk) of specimens 1.51–1.85 mm (n = 3). Specimens pale yellowish white with violet pigments on distal half of the Ant I to Ant IV, head laterally, margins of Th II–Abd II, Abd III with one transverse band that expands laterally, Abd IV dorsally with one irregular lateral spot and one weak central spot, irregular spots on dorsoventral plate and posterior margin; distal half of Abd V to VI, distal femur and tibiotarsus medially; eyepatches black (Fig. 8). Sometimes depigmented on proximal part of the Ant II; pigments on posterior one third of the Th II and Abd I, almost all Abd II–III medially, and posterior half of Abd IV (see Katz 2017: 551).

HEAD. Antennal ratio as I: II: III: IV = 1: 1.83–2.00: 1.68–2.12: 1.81–2.36 (n = 3). Ant IV not annulated, with apical bulb simple or bilobed, rarely retracted. Six interocular chaetae (q, v, s, p, r, t); head dorsal macrochaetotaxy (Fig. 9A) with 5 'An' (An1a–3), 4 'A' (A0, A2–3, A5), 3 'M' (M1–2, M4), 6–7 'S' (S0, S2–6), 0 'Ps', 5 'Pa' (Pa1–5), 2 'Pm' (Pm1, Pm3), 4 'Pp' (Pp1–3, Pp5), and 4 'Pe' (Pe2–3 plus 1 unnamed) mac; An2a?, A1, A4? mic absent. Maxillary palp with t.a. smooth and b.c. weakly striated, thicker and 1.10 longer than t.a.; sublobal plate with 3 inner (sb.1–3) and 1 outer (sb.4) smooth appendages, sb.1 gently smaller, sb.3 thin, and sb.4 minute (Fig. 9B). Ventral chaetotaxy with about 74 ciliate chaetae, 23 thin, 18 slightly smaller, and 33 normal and subequal in length (including b.c.), cephalic groove with 8 chaetae; postlabial formula with 4 (G1–4), 4 (X, X2–4), 4 (H2–4), 4 (J1–4), 2 (X', X4') chaetae (Fig. 9C).

THORAX CHAETOTAXY (as Fig. 6A). Th II and III similar to *W. nigromaculata*, except Th III p2a mac always present. Ratio Th II: III = 1.48–1.30: 1 (n = 3), holotype 1.30: 1.

ABDOMEN CHAETOTAXY (as Figs 6B–F and 9D). Abd I to IV similar to *W. nigromaculata*, except Abd I m2 smaller in length and socket size, Abd II a5 and m2 bothriotricha with 8–9 and 6 accessory chaetae, Abd III m2 bothriotrichum with 3–4 accessory chaetae and a5 and m5 bothriotricha with 12–15 accessory chaetae between them, and Abd IV T2 and T4 bothriotricha with 2 mic and 8–11 accessory chaetae between them. Abd V a, m and p series with 1 (a5), 4 (m2–3, m5–5e), and 5 (p1, p3–6) mac, respectively (Fig. 9D). Ratio Abd III: IV = 1: 3.61–4.14 (n = 3), holotype 1: 3.80.

CHAETOTAXY OF THE LEGS AND COLLOPHORE. Similar to *W. nigromaculata* (Fig. 7A–F).

FURCULA. Manubrium ventrally similar to *W. nigromaculata* (as Figs 4C, 7I); dorsally with one lateral row of 9 ciliate chaetae abruptly acuminate at the tip, 3 mac and 6 mes (2 basal and 2 antero-subapical); manubrial plate with 4 ciliate chaetae of different sizes (2 mac abruptly acuminate at the tip) and 2 psp (Fig. 9E).

DNA Barcodes

GenBank KM610130; collection locality information same as holotype (Katz *et al.* 2015a). GenBank MG034057; Brockville, Canada (deWaard *et al.* 2019).

Remarks

Willowsia neonigromaculata sp. nov. is considered a new species that is distinct from *W. nigromaculata*, supported by both morphological (Table 2) and molecular evidence (Table 3, Figs 10–11). *Willowsia neonigromaculata* sp. nov. resembles *W. nigromaculata* in most morphological characteristics, but differs in head by cephalic mac Ps5 and Pp4 absent and Pe4 plus one extra mac present (opposite in *W. nigromaculata*), 3 mic (An2a?, A1, A4?) absent (present in *W. nigromaculata*) and interocular s chaetae present (absent in *W. nigromaculata*), sublobal plate with 3 inner appendages (2 in *W. nigromaculata*), and ventral groove with 8 chaetae (6 in *W. nigromaculata*). On Abd I, m2 mac for *Willowsia neonigromaculata* sp. nov. smaller in length and socket size than m3 and m4 (normal in *W. nigromaculata*), and Abd V with 3 chaetae (m5ea, p5a, p6e), all absent in *W. nigromaculata*. They also differ in manubrium dorsally with 2 basal and 2 antero-subapical chaetae abruptly acuminate at the tip (1 basal and 1 antero-subapical in *W. nigromaculata*), and manubrial plate with 2 inner mac (1 in *W. nigromaculata*).

Genetic analysis

COI p-distances revealed remarkably high levels of genetic variation among specimens identified as *W. nigromaculata*, with p-distances ranging from 0% to 13.47% (Table 3). Moreover, there is a large gap in the distribution of genetic distances (0–1.18% and 9–13.47%, respectively) (Fig. 10), corresponding to the separation of two phylogenetically distinct lineages within *W. nigromaculata* (Fig. 11). Distances between these two clades (Fig. 10, line C) are similar to distances between other Entomobryinae species (Fig. 10, line A) and distances between Entomobryinae sister taxa (Fig. 10, line B).

Both Bayesian and maximum likelihood phylogenetic approaches produced mostly congruent gene tree topologies, with lineages of the *W. nigromaculata* forming two distinct clades with high support (Fig. 11): (1) a *W. neonigromaculata* sp. nov. clade that includes sequences representing *W. neonigromaculata* sp. nov. collected from Dixon Springs, Illinois, USA and Brockville, Canada (previously identified as *W. nigromaculata*); and (2) a *W. nigromaculata* clade that includes *W. nigromaculata* sequences from specimens collected in Teillet, France and Toronto, Canada. Phylogenetic divergence between these two clades is similar to that observed between other Entomobryinae sister species (Fig. 11).

Discussion

Cryptic species are thought to comprise a vast majority of springtail diversity (Porco *et al.* 2012; Cicconardi *et al.* 2013), which has contributed to the rise of studies that focus on integrating morphological and molecular data to delimit cryptic species within various groups of Collembola (e.g., Zhang *et al.* 2014c, 2018, 2019; Katz *et al.* 2015a; Sun *et al.* 2017; Skarzyński *et al.* 2018; Yu *et al.* 2018; Carapelli *et al.* 2020). Likewise, we provide both morphological and molecular evidence that lineages of *Willowsia nigromaculata* comprise at least two species – *W. neonigromaculata* sp. nov. in North America and *W. nigromaculata* in France and Canada, but also reported throughout the Holarctic realm. Morphological analysis revealed a number of subtle, yet significant differences in chaetotaxy between the two species (Table 2), including the number of inner appendages on the maxillary sublobal plate (Figs 5E, 9B) – a character thought to

Table 2. Morphological comparison between *Willowsia nigromaculata* (Lubbock, 1873) and *W. neonigromaculata* sp. nov. ('+' is present; '−' is absent).

Character	Species		
	<i>W. nigromaculata</i> France	<i>W. neonigromaculata</i> sp. nov. USA	
Cephalic dorsal macrochaetotaxy	S0 Ps5 Pp4 Pe4 Pe extra	+ + + − −	+/- − − + +
Number of interocular chaetae		5	6
Inner appendages on maxillary sublobal plate		2	3
Postlabial chaetotaxy	X, X' X3, X4' groove b.c.	mic mic 6 larger	mes mes 8 normal
Th II–Abd IV mac formula		9,8 3,3,3 + 7,7+14	9,8 3,3,3+7,7 + 14
Abd V chaetotaxy	m5ea p5a p6ai p6e	− − mac −	+ + mes +
Manubrium ventral chaetotaxy	basal antero-subapical subapical	1 2 6	2 1 4
Manubrial plate	number mac	3–4 1	4 2

be highly conserved across Entomobryinae (Katz 2017). The presence of only 2 inner appendages for *W. nigromaculata* from France is surprising, given that to date, only three other species of Entomobryinae are known to share this character state: *Americabrya arida* (Christiansen & Bellinger, 1980), *Willowsia mexicana* Zhang, Palacios-Vargas & Chen, 2007, and *Willowsia pyrrhopygia* Katz, 2017 – all of which are endemic to the New World (Katz 2017). However, until recently, this character was rarely reported in the literature, so it is possible that 2 inner appendages may be more common than previously thought.

The recovery of two highly supported and phylogenetically distinct clades (Fig. 11), separated by approximately 13% sequence divergence (Table 3; Fig. 10), provides additional support for our new species designation. However, the presence of both species in Canada indicates that the distribution of diversity in this group does not seem to correspond with geography. Extremely low levels of sequence divergence (approx. 1%) observed between *W. nigromaculata* specimens collected in France and Toronto, Canada (Table 3) are indicative of a recent range expansion via trans-Atlantic dispersal, possibly facilitated by *W. nigromaculata*'s strong association with human structures. As expected, the phylogenetic analysis also supports previous observations of para-/polyphyletic genera within Entomobryinae (Zhang *et al.* 2014a, 2014b, 2015, 2016, 2017; Katz *et al.* 2015b, 2017; Zhang &

Deharveng 2015; Ding *et al.* 2018), though the primary objective of this study was to assess genetic diversity within *Willowsia*, not to resolve generic relationships within Entomobryinae – a task that will likely require large, genomic data sets.

We consider the specimen identified as *W. nigromaculata* from Brockville, Ontario, Canada (deWaard *et al.* 2019), as a synonym of *W. neonigromaculata* sp. nov. based on genetic similarity (0.18% COI sequence divergence). Sequence divergence in COI seems to accumulate long before obvious morphological divergence in springtails, with cryptic species often having >8% sequence divergence in COI (Porco *et al.* 2012; Cicconardi *et al.* 2013; Katz *et al.* 2015a). Nevertheless, future morphological analysis of Canadian specimens would provide additional support for the presence of *W. neonigromaculata* sp. nov. in Canada.

In light of these results, we expect that specimens previously identified as *W. nigromaculata*, especially those collected in the USA and Canada, may actually be *W. neonigromaculata* sp. nov. and the reexamination of old material may reveal additional new species. Additional morphological and molecular investigations of specimens collected throughout the Holarctic region are needed to better understand the diversity and distribution of *W. nigromaculata* and *W. neonigromaculata* sp. nov.

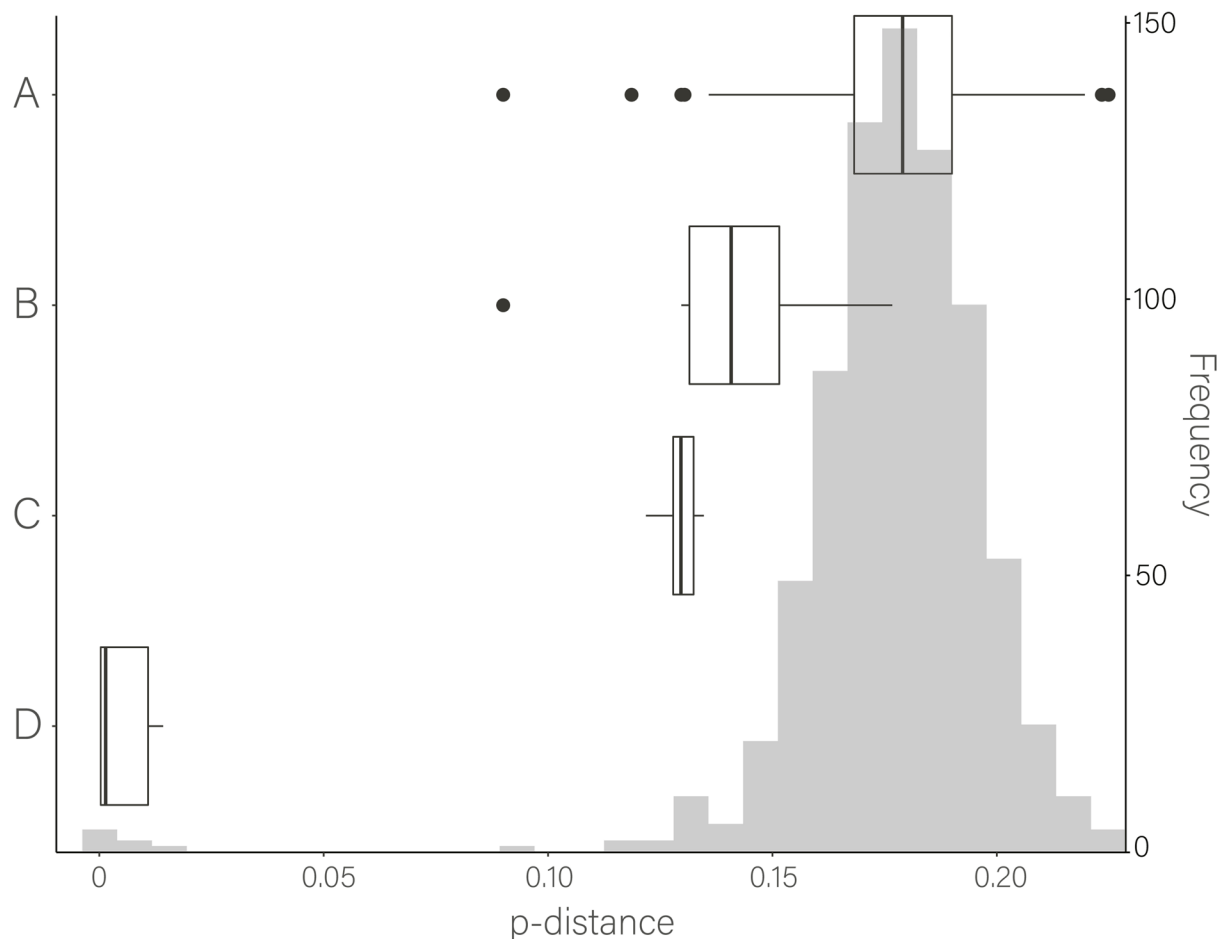


Fig. 10. COI p-distance (uncorrected) frequency histogram (in gray) and boxplots comparing p-distances between **A**. Entomobryinae species. **B**. Entomobryinae sister species. **C**. *Willowsia nigromaculata* (Lubbock, 1873) (France and Toronto, Canada) and *W. neonigromaculata* sp. nov (USA and Brockville, Canada) clades (inter-specific distances). **D**. Lineages within the same *W. nigromaculata* or *W. neonigromaculata* sp. nov. clade (intra-specific distances).

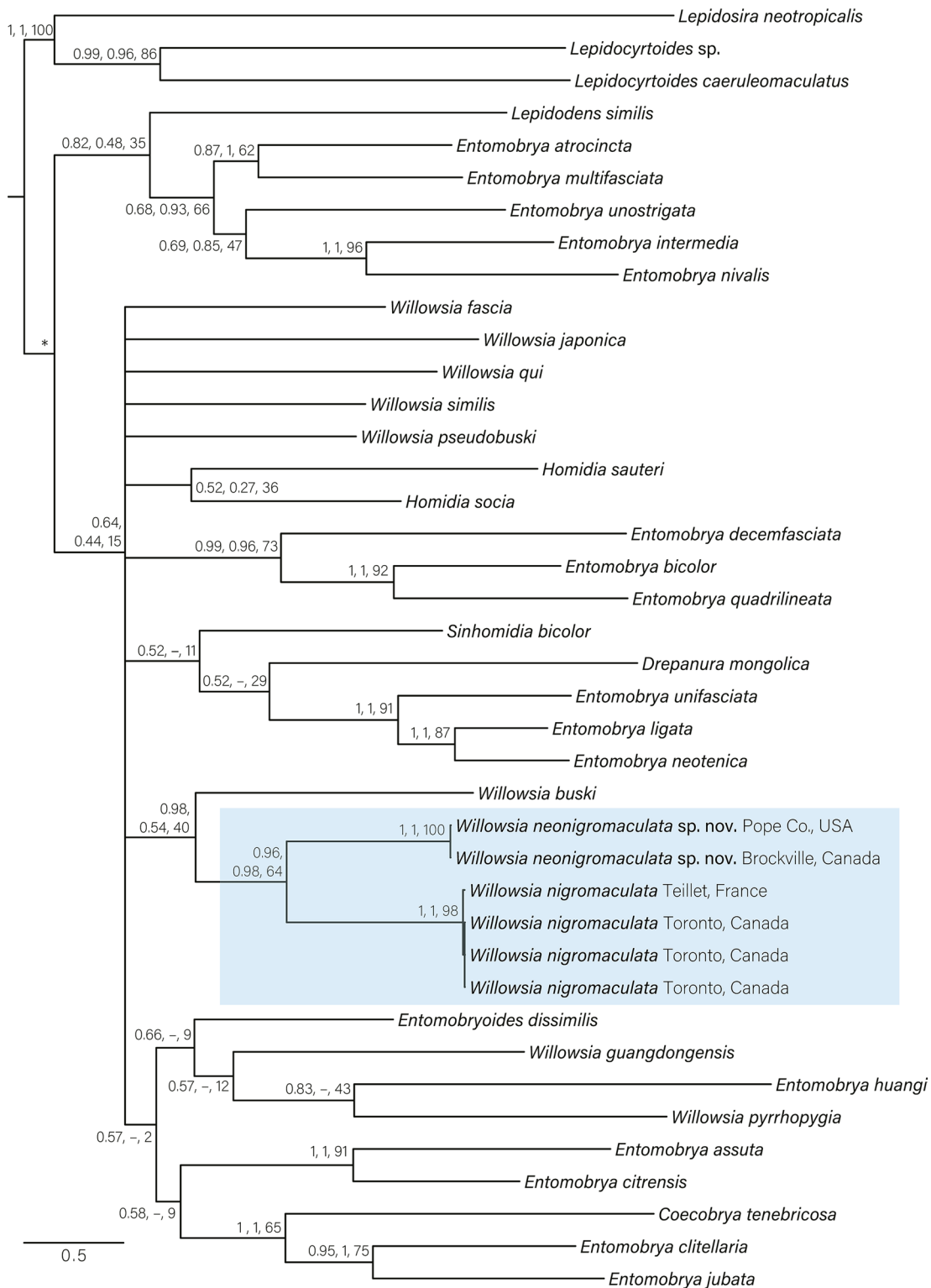


Fig. 11. Bayesian consensus tree estimated with MrBayes for Entomobryinae, including the clade comprised of *Willowsia nigromaculata* (Lubbock, 1873) from France and Canada and *W. neonigromaculata* sp. nov. from the USA and Canada (highlighted). MrBayes and BEAST posterior probabilities and RAxML bootstraps are indicated at each node, respectively. The ingroup node constrained as monophyletic for all phylogenetic analyses is indicated with an asterisk (*).

Table 3. COI p-distances between *Willowsia nigromaculata* (Lubbock, 1873) and *W. neonigromaculata* sp. nov. References: Katz *et al.* 2015a¹; Ding *et al.* 2018²; deWaard *et al.* 2019³. Abbreviations: CA = Canada; FR = France.

Species name	Locality	COI GenBank accession #	<i>Willowsia</i>				
			<i>neonigromacu-</i> <i>ta</i> sp. nov. USA KM610130 ⁽¹⁾	<i>nigromacu-</i> <i>lata</i> France KY468311	<i>nigromacu-</i> <i>lata</i> Toronto MG032239	<i>nigromacu-</i> <i>lata</i> Toronto MG036766	<i>nigromacu-</i> <i>lata</i> Toronto MG039377
<i>W. nigromaculata</i>	Tiellet, FR	KY468311 ²	12.92%				
	Toronto, CA	MG032239 ³		12.05%	1.06%		
	Toronto, CA	MG036766 ³		13.03%	1.18%	0.00%	
	Toronto, CA	MG039377 ³		13.10%	1.11%	0.00%	0.00%
	Brock- ville, CA	MG034057 ³	0.18%	13.47%	12.26%	12.93%	12.99%

Acknowledgments

We would like to thank Dr Vitor D. Tarli (MNHN) who supplied us the material described in this study, Dr Feng Zhang (Nanjing Agricultural University) for molecular data communication, CAPES Pro-Equipamentos (Dra Neusa Hamada/INPA), Laboratório de Sistemática e Ecologia de Invertebrados do Solo (Dra. Elizabeth F. Chilson/INPA) and Laboratório Temático de Microscopia Óptica e Eletrônica (LTMOE/ INPA, by J. Veras, L. Castanhola, and J.W. Meirelles) for logistic support with the images, and Daniel R. Swanson (University of Illinois at Urbana-Champaign) for his etymological expertise. The first author's post-doctoral appointment is granted by CNPq (PCI-DB, Process # 300925/2019-0).

References

- Bellinger P.F., Christiansen K.A. & Janssens F. 2020. *Checklist of the Collembola of the World*. Available from <http://www.collembola.org> [accessed 20 Apr. 2020].
- Bouckaert R. & Drummond A. 2017. bModelTest: Bayesian phylogenetic site model averaging and model comparison. *BMC Evolutionary Biology* 17: 42. <https://doi.org/10.1186/s12862-017-0890-6>
- Bouckaert R., Vaughan T.G., Barido-Sottani J., Duchêne S., Fourment M., Gavryushkina A., Heled J., Jones G., Kühnert D., De Maio N., Matschiner M., Mendes F.K., Müller N.F., Huw A. Ogilvie H.A., du Plessis L., Popinga A., Rambaut A., Rasmussen D., Siveroni I., Suchard M.A., Wu C.-H., Xie D., Zhang C., Stadler T. & Drummond A.J. 2019. BEAST 2.5: An advanced software platform for Bayesian evolutionary analysis. *PLoS Computational Biology* 15 (4): e1006650. <https://doi.org/10.1371/journal.pcbi.1006650>
- Carapelli A., Greenslade P., Nardi F., Leo C., Convey P., Frati F. & Fanciulli P.P. 2020. Evidence for the cryptic diversity in the “Pan-Antarctic” springtail *Friesea antarctica* and the description of two new species. *Insects* 11 (3): 141. <https://doi.org/10.3390/insects11030141>
- Chen J.-X. & Christiansen K.A. 1993. The genus *Sinella* with special reference to *Sinella s. s.* (Collembola: Entomobryidae) of China. *Oriental Insects* 27: 1–54.

Christiansen K. & Bellinger P. 1980. *The Collembola of North America, North of the Rio Grande: A Taxonomic Analysis*. Grinnell College, Grinnell, Iowa.

Christiansen K. & Bellinger P. 1998. *The Collembola of North America, North of the Rio Grande: A Taxonomic Analysis*. Grinnell College, Grinnell, Iowa.

Cicconardi F., Fanciulli P.P. & Emerson B.C. 2013. Collembola, the biological species concept and the underestimation of global species richness. *Molecular Ecology* 22 (21): 5382–5396.
<https://doi.org/10.1111/mec.12472>

Cipola N.G., Moraes J.W. & Bellini B.C. 2014. A new species of *Seira* (Collembola: Entomobryidae: Seirini) from Northern Brazil, with the addition of new chaetotaxic characters. *Zoologia* 31: 489–495.
<https://doi.org/10.1590/S1984-46702014000500009>

Cipola N.G., Oliveira J.V.L.C., Bellini B.C., Ferreira A.S., Lima E.C.A., Brito R.A., Stievano L.C., Souza P.G. & Zeppelini D. 2020. Review of eyeless *Pseudosinella* Schäffer (Collembola, Entomobryidae, Lepidocyrtinae) from Brazilian caves. *Insects* 11: 1–140. <https://doi.org/10.3390/insects11030194>

deWaard J.R., Ratnasingham S., Zakharov E.V., Borisenko A.V., Steinke D., Telfer A.C., Perez K.H.J., Sones J.E., Monica R. Young M.R., Valerie Levesque-Beaudin V., Crystal N. Sobel C.N., Abrahamyan A., Bessonov K., Blagoev G., deWaard S.L., Ho C., Ivanova N.V., Layton K.K.S., Lu L., Manjunath R., McKeown J.T.A., Milton M.A., Miskie R., Monkhouse N., Naik S., Nikolova N., Pentinsaari M., Prosser S.W.J., Radulovici A.E., Steinke C., Warne C.P. & Hebert P.D.N. 2019. A reference library for Canadian invertebrates with 1.5 million barcodes, voucher specimens, and DNA samples. *Scientific Data* 6: 308. <https://doi.org/10.1038/s41597-019-0320-2>

Ding Y.-H., Yu D.-Y., Guo W.-B., Li J.-N. & Zhang F. 2018. Molecular phylogeny of *Entomobrya* (Collembola: Entomobryidae) from China: Color pattern groups and multiple origins. *Insect Science* 26 (3): 587–597. <https://doi.org/10.1111/1744-7917.12559>

Fjellberg A. 1999. The Labial Palp in Collembola. *Zoologischer Anzeiger* 237: 309–330.

Fjellberg A. 2007. *The Collembola of Fennoscandia and Denmark, Part II: Entomobryomorpha and Symphyleona*. Fauna Entomologica Scandinavica Volume 42, Brill, Leiden.

Gisin H. 1960. *Collembolenfauna Europas*. Museum D'Histoire naturelle, Genève.

Gisin H. 1967. Espèces nouvelles et lignées évolutives de *Pseudosinella* endogés. *Memórias e Estudos do Museu Zoológico da Universidade de Coimbra* 301: 5–25.

Godeiro N.N., Pacheco G., Liu S., Cipola N.G., Berbel-Filho W.M., Zhang F., Gilbert M.T.P. & Bellini B.C. 2020. Phylogeny of Neotropical Seirinae (Collembola, Entomobryidae) based on mitochondrial genomes. *Zoologica Scripta* 49 (3): 329–339. <https://doi.org/10.1111/zsc.12408>

Guthrie J.E. 1903. *The Collembola of Minnesota*. Zoological Series IV, Geological and Natural History Survey of Minnesota, Minneapolis, Minnesota. <https://doi.org/10.5962/bhl.title.1701>

Hüther W. 1986. New aspects in taxonomy of *Lepidocyrtus* (Collembola). In: Dallai R. (ed.) 2nd International Seminar on Apterygota: 61–65. University of Siena, Siena.

Jordana R. 2012. Synopses of Palaearctic Collembola: Capbryinae & Entomobryini. *Soil Organisms* 84 (1): 1–390.

Jordana R., Arbea J.I., Simón C. & Luciáñez M.J. 1997. *Fauna Iberica, Vol. 8. Collembola Poduromorpha*. Museo Nacional de Ciencias Naturales, Madrid.

Katoh K. & Standley D.M. 2013. MAFFT multiple sequence alignment software version 7: improvements in performance and usability. *Molecular Biology and Evolution* 30 (4): 772–780.

<https://doi.org/10.1093/molbev/mst010>

Katz A.D. 2017. A new endemic species of *Willowsia* from Florida (USA) and descriptive notes on all New World *Willowsia* (Collembola: Entomobryidae). *Zootaxa* 4350 (3): 549–562.

<https://doi.org/10.11646/zootaxa.4350.3.7>

Katz A.D., Giordano R. & Soto-Adames F.N. 2015a. Operational criteria for cryptic species delimitation when evidence is limited, as exemplified by North American *Entomobrya* (Collembola: Entomobryidae). *Zoological Journal of the Linnean Society* 173 (4): 810–840. <https://doi.org/10.1111/zoj.12220>

Katz A.D., Giordano R. & Soto-Adames F. 2015b. Taxonomic review and phylogenetic analysis of fifteen North American *Entomobrya* (Collembola, Entomobryidae), including four new species. *ZooKeys* 525: 1–75. <https://doi.org/10.3897/zookeys.525.6020>

Kawada R. & Buffington M.L. 2016. A scalable and modular dome illumination system for scientific microraphy on a budget. *PLoS ONE* 11 (5): 1–20. <https://doi.org/10.1371/journal.pone.0153426>

Kozlov A.M., Darriba D., Flouri T., Morel B. & Stamatakis A. 2019. RAxML-NG: a fast, scalable and user-friendly tool for maximum likelihood phylogenetic inference. *Bioinformatics* 35 (21): 4453–4455. <https://doi.org/10.1093/bioinformatics/btz305>

Lanfear R., Frandsen P.B., Wright A.M., Senfeld T. & Calcott B. 2017. PartitionFinder 2: New methods for selecting partitioned models of evolution for molecular and morphological phylogenetic analyses. *Molecular Biology and Evolution* 34 (3): 772–773. <https://doi.org/10.1093/molbev/msw260>

Lubbock J. 1873. *Monograph of the Collembola and Thysanura*. Ray Society, London.
<https://doi.org/10.5962/bhl.title.11583>

Mari-Mutt J.A. 1979. A revision of the genus *Dicranocentrus* Schött (Insecta: Collembola: Entomobryidae). *Agricultural Experiment Station Bulletin* 259: 1–79.

Maynard E.A. 1951. *A Monograph of the Collembola or Springtail Insects of New York State*. Comstock Publishing Company, Inc., Ithaca, New York.

Nunes R.C., Godeiro N.N., Pacheco G., Liu S., Gilbert M.T.P., Alvarez Valin F., Zhang F. & Bellini B.C. 2019. The discovery of Neotropical *Lepidosira* (Collembola, Entomobryidae) and its systematic position. *Zoologica Scripta* 48 (6): 783–800. <https://doi.org/10.1111/zsc.12377>

Porco D., Bedos A., Greenslade P., Janion-Scheepers C., Skarżyński D., Stevens M.I., Jansen van Vuuren B. & Deharveng L. 2012. Challenging species delimitation in Collembola: cryptic diversity among common springtails unveiled by DNA barcoding. *Invertebrate Systematics* 26: 470–477.
<https://doi.org/10.1071/IS12026>

R Core Team. 2020. *R: A Language and Environment for Statistical Computing*. R Foundation for Statistical Computing, Vienna, Austria. Available from (<https://www.R-project.org/>) [accessed 5 May 2020]

Rambaut A., Drummond A.J., Xie D., Baele G. & Suchard M.A. 2018. Posterior summarisation in Bayesian phylogenetics using Tracer 1.7. *Systematic Biology* 67 (5): 901–904.
<https://doi.org/10.1093/sysbio/syy032>

Ronquist F., Teslenko M., Van Der Mark P., Ayres D.L., Darling A., Höhna S., Larget B., Liu L., Suchard M.A. & Huelsenbeck J.P. 2012. MrBayes 3.2: efficient Bayesian phylogenetic inference and model choice across a large model space. *Systematic Biology* 61 (3): 539–542.
<https://doi.org/10.1093/sysbio/sys029>

Scott H.G. 1991. Springtails. In: Gorham S.J. (ed.) *Insect and Mite Pests in Food: an Illustrated Key. Part 2*: 351–361. Agriculture Handbook 655, United States Department of Agriculture, Washington, D.C.

Shoebottom J.W. 1917. Notes on the Collembola, part 4. The classification of the Collembola; with a list of genera known to occur in the British Isles. *Annals and Magazine of Natural History series* 19: 425–436. <https://doi.org/10.1080/00222931709486959>

Skarżyński D., Piwnik, A. & Porco D. 2018. Integrating morphology and DNA barcodes fro species delimitation within the species complex *Xenylla maritima* (Collembola: Hypogastruridae). *Arthropod Systematics & Phylogeny* 76 (1): 31–43.

Soto-Adames F.N. 2002. Molecular phylogeny of the Puerto Rican *Lepidocyrtus* and *Pseudosinella* (Hexapoda: Collembola), a validation of Yoshii's "color pattern species". *Molecular Phylogenetics and Evolution* 25 (1): 27–42. [https://doi.org/10.1016/S1055-7903\(02\)00250-6](https://doi.org/10.1016/S1055-7903(02)00250-6)

Soto-Adames F.N. 2008. Postembryonic development of the dorsal chaetotaxy in *Seira dowlingi* (Collembola, Entomobryidae); with an analysis of the diagnostic and phylogenetic significance of primary chaetotaxy in *Seira*. *Zootaxa* 1683 (1): 1–31. <https://doi.org/10.11646/zootaxa.1683.1.1>

Stach J. 1967. Collembola fauna of Malta. *Acta Zoologica Cracoviensis* 12 (15): 393–418.

Sun X., Zhang F., Ding Y., Davies T.W., Li Y. & Wu D. 2017. Delimiting species of *Protaphorura* (Collembola: Onychiuridae): integrative evidence based on morphology, DNA sequences and geography. *Scientific Reports* 7: 8261. <https://doi.org/10.1038/s41598-017-08381-4>

Szeptycki A. 1979. *Chaetotaxy of the Entomobryidae and its phylogenetical Significance. Morpho-systematic Studies on Collembola. IV*. Polska Akademia Nauk, Karków.

Yoshii R. & Suhardjono Y.R. 1992. Collembolan fauna of Indonesia and its affinities III: Collembola of Timor Island. *Acta Zoologica Asiae Orientalis* 2: 75–96.

Yosii R. 1959. Studies on the Collembolan fauna of Malay and Singapore with special reference to the genera: *Lobella*, *Lepidocyrtus* and *Callyntrura*. *Contributions from the Biological Laboratory Kyoto University* 10: 1–65.

Yu D., Qin C., Ding Y., Hu F., Zhang F. & Liu M. 2018. Revealing species diversity of *Tomocerus ocreatus* complex (Collembola: Tomoceridae): integrative species delimitation and evaluation of taxonomic characters. *Arthropod Systematics & Phylogeny* 76 (1): 147–172.

Zhang F. & Deharveng L. 2015. Systematic revision of Entomobryidae (Collembola) by integrating molecular and new morphological evidence. *Zoologica Scripta* 44 (3): 298–311.

<https://doi.org/10.1111/zsc.12100>

Zhang F., Palacios-Vargas J.G. & Chen J.-X. 2007. The genus *Willowsia* and its Mexican species (Collembola: Entomobryidae). *Annals of the Entomological Society of America* 100 (1): 36–40. [https://doi.org/10.1603/0013-8746\(2007\)100\[36:TGWAIM\]2.0.CO;2](https://doi.org/10.1603/0013-8746(2007)100[36:TGWAIM]2.0.CO;2)

Zhang F., Chen J.-X. & Deharveng L. 2011. New insight into the systematics of the *Willowsia* complex (Collembola: Entomobryidae). *Annales de la Société entomologique de France* 47: 1–20. <https://doi.org/10.1080/00379271.2011.10697692>

Zhang F., Bedos A. & Deharveng L. 2014a. Disjunct distribution of *Szeptyckiella* gen. nov. from New Caledonia and South China undermines the monophyly of Willowsiini (Collembola: Entomobryidae). *Journal of Natural History* 48 (21–22): 1299–1317. <https://doi.org/10.1080/00222933.2013.859317>

Zhang F., Chen Z., Dong R.R., Deharveng L., Stevens M.I., Huang Y.H. & Zhu C.D. 2014b. Molecular phylogeny reveals independent origins of body scales in Entomobryidae (Hexapoda: Collembola). *Molecular Phylogenetics and Evolution* 70: 231–239. <https://doi.org/10.1016/j.ympev.2013.09.024>

Zhang F., Yu D., Luo Y., Ho S.Y.W., Wang B. & Zhu C. 2014c. Cryptic diversity, diversification and vicariance in two species complexes of *Tomocerus* (Collembola, Tomoceridae) from China. *Zoologica Scripta* 43 (4): 393–404. <https://doi.org/10.1111/zsc.12056>

Zhang F., Sun D.D., Yu D.Y. & Wang B.X. 2015. Molecular phylogeny supports S-chaetae as a key character better than jumping organs and body scales in classification of Entomobryoidea (Collembola). *Scientific Reports* 5: 1–12. <https://doi.org/10.1038/srep12471>

Zhang F., Pan Z., Wu J., Ding Y., Yu D. & Wang B. 2016. Dental scales could occur in all scaled subfamilies of Entomobryidae (Collembola): new definition of Entomobryinae with description of a new genus and three new species. *Invertebrate Systematics* 30 (6): 598–615.

<https://doi.org/10.1071/IS16005>

Zhang F., Ma Y. & Greenslade P. 2017. New Australian Paronellidae (Collembola) reveal anomalies in existing tribal diagnoses. *Invertebrate Systematics* 31 (4): 375–393. <https://doi.org/10.1071/IS16073>

Zhang F., Yu D., Stevens M.I. & Ding Y. 2018. Colouration, chaetotaxy and molecular data provide species-level resolution in a species complex of *Dicranocentrus* (Collembola: Entomobryidae). *Invertebrate Systematics* 32:1298–1315. <https://doi.org/10.1071/IS18019>

Zhang B., Chen T.-W., Mateos E., Scheu S. & Schaefer I. 2019. DNA-based approaches uncover cryptic diversity in the European *Lepidocyrtus lanuginosus* species group (Collembola: Entomobryidae). *Invertebrate Systematics* 33 (4): 661–670. <https://doi.org/10.1071/IS18068>

Manuscript received: 13 May 2020

Manuscript accepted: 10 December 2020

Published on: 16 March 2021

Topic editor: Nesrine Akkari

Desk editor: Marianne Salaün

Printed versions of all papers are also deposited in the libraries of the institutes that are members of the *EJT* consortium: Muséum national d'histoire naturelle, Paris, France; Meise Botanic Garden, Belgium; Royal Museum for Central Africa, Tervuren, Belgium; Royal Belgian Institute of Natural Sciences, Brussels, Belgium; Natural History Museum of Denmark, Copenhagen, Denmark; Naturalis Biodiversity Center, Leiden, the Netherlands; Museo Nacional de Ciencias Naturales-CSIC, Madrid, Spain; Real Jardín Botánico de Madrid CSIC, Spain; Zoological Research Museum Alexander Koenig, Bonn, Germany; National Museum, Prague, Czech Republic.

ZOBODAT - www.zobodat.at

Zoologisch-Botanische Datenbank/Zoological-Botanical Database

Digitale Literatur/Digital Literature

Zeitschrift/Journal: [European Journal of Taxonomy](#)

Jahr/Year: 2021

Band/Volume: [0739](#)

Autor(en)/Author(s): Cipola Nikolas G., Katz Aron D.

Artikel/Article: [Morphological and molecular analysis of Willowsia nigromaculata \(Collembola, Entomobryidae, Entomobryinae\) reveals a new cryptic species from the United States 92-116](#)